

Direct Photons at RHIC

Klaus Reygers¹ for the PHENIX Collaboration

¹Physikalisches Institut, Universität Heidelberg, Philosophenweg 12, 69120 Heidelberg, Germany

DOI: will be assigned

A brief overview of direct-photon measurements in p+p and Au+Au collisions at $\sqrt{s_{NN}} = 200$ GeV with the PHENIX experiment at the Relativistic Heavy Ion Collider (RHIC) is given. Direct-photon yields for $p_T \gtrsim 4$ GeV/c and photon-hadron azimuthal correlations were determined with the aid of an electromagnetic calorimeter. By detecting e^+e^- pairs from the internal conversion of virtual photons direct-photon yields were measured between $1 \lesssim p_T \lesssim 4$ GeV/c. In Au+Au collisions thermal photons from a quark-gluon plasma (QGP) are expected to contribute significantly to the total direct-photon yield in this range.

1 Introduction

In heavy-ion physics direct photons are typically defined as the difference between all measured photons and background photons from hadronic decays [1]. Thus, isolated prompt photons with small hadronic activity around them accompanied by a jet on the away-side as well as photons produced in the fragmentation of jets (fragmentation photons) contribute to the direct-photon signal. The primary reason for the interest in direct photons is their large mean free path with respect to the dimensions of the created fireball. Thus, once produced photons leave the fireball unscathed and carry away information about the early stage of the collisions.

The measured direct-photon signal is an integral over the entire evolution of the fireball where different processes are dominant at different times. This is often regarded as a virtue, however, it also means that disentangling the different sources typically relies on comparisons with model calculations. The production of direct photons in ultra-relativistic A+A collision can be divided into the following stages [2]. At first, direct photons are produced in initial hard parton scatterings analogous to the production mechanism in p+p collisions. The yield of these photons can be calculated in perturbative QCD and they are the dominant direct-photon source at high p_T ($p_T \gtrsim 6$ GeV/c for Au+Au at $\sqrt{s_{NN}} = 200$ GeV). After a time on the order of $\tau_0 \approx 1$ fm/c [3] it is expected that a medium of deconfined quarks and gluons (the quark-gluon plasma) forms for which a local temperature is a meaningful concept. In such a thermalized medium thermal direct photons will be produced whose momentum distribution reflects the temperature of the system. At a temperature of $T_c \approx 140 - 200$ MeV [4, 5] a transition to a hot hadron gas takes place and thermal direct photons are also produced in this phase.

It was discovered at RHIC that quark and gluon jets in central A+A collisions are affected by the created medium. Jets apparently lose energy which results, *e.g.*, in a reduced yield of pions at high p_T [6]. This is referred to as jet quenching. The jet-medium interaction gives rise to further sources of direct photons. First, a direct photon can be produced in so-called

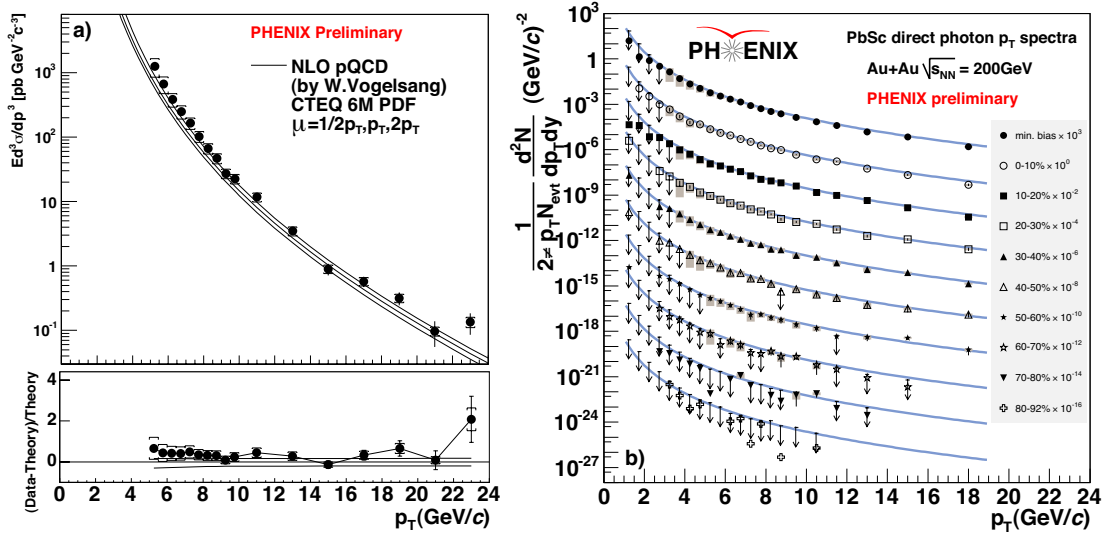


Figure 1: a) Direct-photon invariant cross section in p+p collisions at $\sqrt{s} = 200$ GeV from the 2005 run. The data agree with a next-to-leading-order (NLO) QCD calculation. Final data from 2003 run were published in [9]. b) Direct-photons yields in Au+Au collisions at $\sqrt{s_{NN}} = 200$ GeV from the 2004 run for various centralities. The data are compared a p+p NLO QCD calculation scaled by $\langle T_{AB} \rangle = \langle N_{\text{coll}} \rangle / \sigma_{\text{inel}}^{\text{NN}}$. Final results from the 2002 run were published in [10].

jet-photon conversions, *e.g.*, in gluon Compton scattering $q_{\text{jet}} + g_{\text{QGP}} \rightarrow q + \gamma$ [7]. In these processes the photon typically carries a large fraction of the initial jet energy. Second, the presence of the medium induces the emission of bremsstrahlung photons [8]. This is analogous to the induced gluon emission which is believed to be the dominant mechanism for the jet energy loss.

2 Direct Photons at High p_T

In the PHENIX experiment direct photons at midrapidity ($|y| < 0.35$) above $p_T \approx 4$ GeV/c are measured with an electromagnetic calorimeter (EMCal) [11]. This detector subtends $\Delta\phi \approx \pi$ in azimuth and consists of highly segmented lead-scintillator sampling (PbSc, 6 sectors) and lead-glass Cherenkov calorimeters (PbGl, 2 sectors). The two detector technologies have different systematics and provide the possibility of internal cross-checks. In the Au+Au analysis the ratio $(\gamma_{\text{inclusive}}/\pi^0)_{\text{meas}}$ of the inclusive photon spectrum, *i.e.*, the spectrum of photon from all sources including decay photons, and the π^0 spectrum is calculated. A direct-photon excess can then be found by dividing this ratio by $(\gamma_{\text{decay}}/\pi^0)_{\text{calc}}$, *i.e.*, by the calculated number of hadronic decay photons per π^0 . The dominant contribution to these background photons comes from $\pi^0 \rightarrow \gamma\gamma$ and $\eta \rightarrow \gamma\gamma$. Extracting the direct-photon excess from the ratio $(\gamma_{\text{inclusive}}/\pi^0)_{\text{meas}}$ has the advantage that uncertainties of the energy scale of the calorimeter partially cancel. The

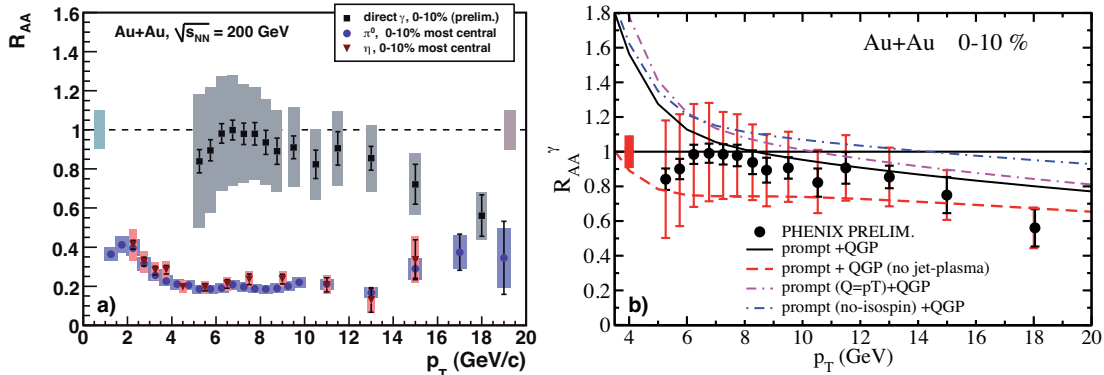


Figure 2: a) R_{AA} in central Au+Au collisions at $\sqrt{s_{NN}} = 200$ GeV for direct photons, π^0 's and η 's. b) Direct-photon data from a) compared to a calculation which as a net result of different nuclear effects discussed in the main text predicts $R_{AA} \approx 0.8$ at $p_T \approx 20$ GeV/c.

direct-photon yield is then calculated as

$$\gamma_{\text{direct}} = \gamma_{\text{inclusive}} - \gamma_{\text{decay}} = (1 - R^{-1}) \times \gamma_{\text{inclusive}} \quad \text{with} \quad R = \frac{(\gamma_{\text{inclusive}}/\pi^0)_{\text{meas}}}{(\gamma_{\text{decay}}/\pi^0)_{\text{calc}}} . \quad (1)$$

In p+p collisions also a slightly different statistical subtraction method is employed [9].

Figure 1a shows that the measured invariant direct-photon cross section in p+p collisions at $\sqrt{s} = 200$ GeV agrees with a next-to-leading-order (NLO) QCD calculation. In the absence of nuclear effects yields of hard scattering processes are expected to scale as $\langle T_{AB} \rangle \times E d^3\sigma/d^3p|_{p+p}$. The nuclear overlap function $\langle T_{AB} \rangle$ reflects the nuclear geometry and is related to the number of inelastic nucleon-nucleon collisions according to $\langle T_{AB} \rangle = \langle N_{\text{coll}} \rangle / \sigma_{\text{inel}}^{\text{NN}}$ where $\sigma_{\text{inel}}^{\text{NN}}$ is the inelastic nucleon-nucleon cross section [12]. The scaled p+p NLO QCD cross section agrees well with the measured direct-photon yields as can be seen in Figure 1b.

The nuclear modification factor

$$R_{AB}(p_T) = \frac{dN/dp_T|_{A+B}}{\langle T_{AB} \rangle \times d\sigma/dp_T|_{p+p}} \quad (2)$$

is used to quantify nuclear effects on the single particle yields. The suppression of the π^0 and η yields by a factor of ~ 5 in central Au+Au collisions at $\sqrt{s_{NN}} = 200$ GeV [6] as shown in Figure 2a is interpreted as the result of energy loss of quark and gluon jets in a medium of high color-charge density. The yield of direct photons from initial hard parton scatterings in A+A collisions is expected to scale with $\langle T_{AB} \rangle$ which is indeed observed in the region $6 \lesssim p_T \lesssim 12$ GeV/c. Thus, the direct-photon results at high p_T support the parton-energy loss interpretation.

At first sight the decrease of the direct photon R_{AA} below unity for $p_T \gtrsim 14$ GeV/c spoils the simple picture of the last paragraph. However, $\langle T_{AB} \rangle$ scaling of direct-photon yields is clearly an oversimplification. First, a Au+Au collision can be regarded as a superposition of p+p, p+n, and n+n collisions whereas only p+p collisions are used as reference in the calculation of R_{AA} . This so-called isospin effect reduces R_{AA} at high p_T . Moreover, the energy loss of jets will lead

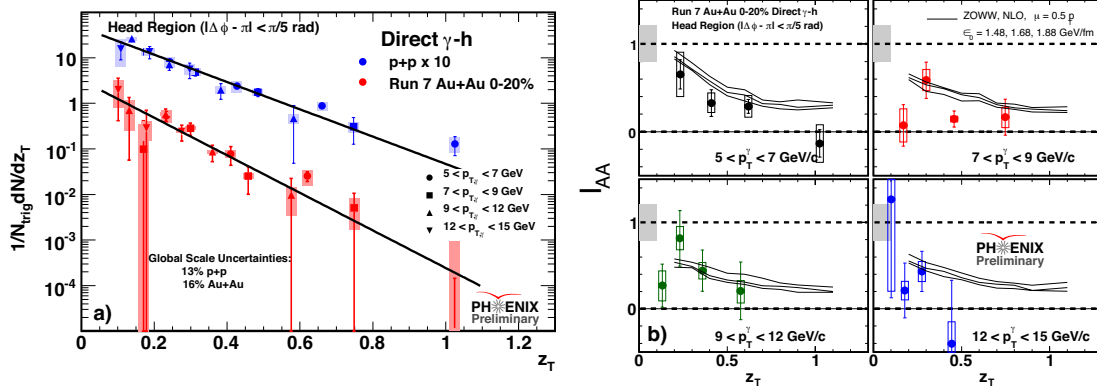


Figure 3: a) Charged-hadron yields opposite to a direct photon as a function of $z_T = p_T^{\text{hadron}}/p_T^\gamma$ in p+p (run 2005 + 2006) and Au+Au (run 2007) at $\sqrt{s_{NN}} = 200$ GeV. b) The ratio $I_{AA} = D_{A+A}(z_T)/D_{p+p}(z_T)$ for four ranges the trigger photon p_T . Results from 2004 Au+Au run are published in [13].

to a reduced production of fragmentation photons. On the other hand, anti-shadowing of the parton distribution in the Au nucleus and bremsstrahlung photons from jet-plasma interactions will increase R_{AA} . In the calculation in Figure 2 the combination of these effects results in an $R_{AA} \approx 0.8$ at $p_T = 20$ GeV/c. The experimental issue here is the correction for the merging of the two showers from $\pi^0 \rightarrow \gamma\gamma$. A detailed study of this effect will be carried out for the final publication.

3 Photon-Triggered Away-side Correlations

The pion yield at high p_T in a given bin at p_T^π results from jets with a large spread in transverse momentum $p_T^{\text{jet}} \gtrsim p_T^\pi$. Thus, the measured pion R_{AA} contains only indirect information about the energy loss of a jet with a given energy. To better constrain the initial jet energy one can study jets opposite ($\Delta\phi \approx \pi$) to a direct photon as for leading order processes $p_T^{\text{jet}} = p_T^\gamma$. Full jet reconstruction is difficult in heavy-ion reactions so that photon-triggered away-side correlations are a useful tool to study jet energy loss. One defines $z_T = p_T^{\text{hadron}}/p_T^\gamma$ and the distribution $D(z_T) = 1/N_\gamma^{\text{trig}} dN^{\text{hadron}}/dz_T$ approximates the light quark fragmentation function [13].

The z_T distributions of charged hadrons associated with a direct photon are shown in Figure 3. If the z_T distribution in p+p collisions is a good approximation of the fragmentation function the distribution should scale in z_T , *i.e.*, it should only depend on z_T independent of the p_T of the trigger photons. This is approximately satisfied in p+p, but interestingly apparently also in Au+Au. The distributions in p+p and Au+Au are fit with an exponential $\exp(-bz_T)$. The difference between p+p ($b = 6.89 \pm 0.64$) and Au+Au ($b = 9.49 \pm 1.37$) reflects the energy loss in the medium.

The ratios $I_{AA} = D_{A+A}(z_T)/D_{p+p}(z_T)$ for different p_T ranges of the trigger photon are shown in Figure 3. They are compared with a jet quenching calculation [14] in which an energy loss parameter was tuned to describe the single particle R_{AA} . Overall a good agreement with the data is observed. However, the uncertainties of the data points are currently too large to

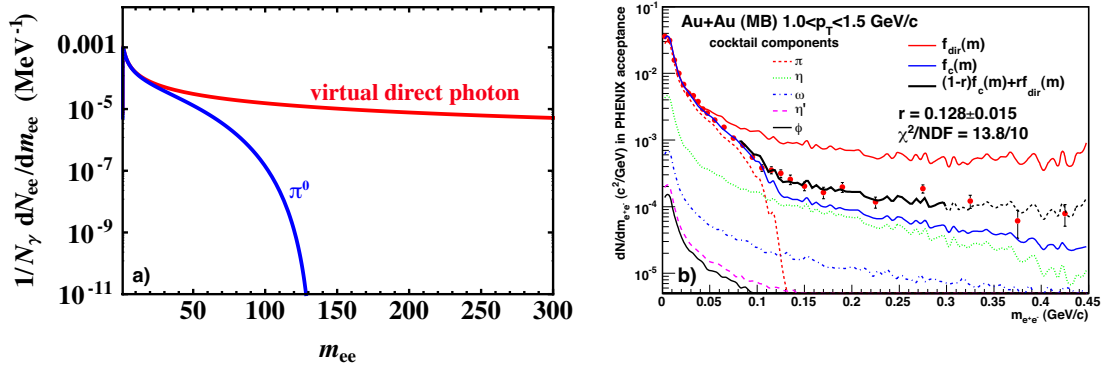


Figure 4: a) Mass distribution of e^+e^- pairs from internal conversion as given by Equation 3. b) Measured e^+e^- mass distribution in Au+Au collisions at $\sqrt{s_{NN}} = 200$ GeV. The data are well described by adding contributions from hadronic decays and virtual direct photons.

confirm the change of I_{AA} with the p_T of the photon trigger as predicted by the calculation.

4 Direct Photons at Low p_T

Systematic uncertainties related to the energy scale, the correction of detector effects and the extraction of the π^0 yields prevent the measurement of direct photons with the PHENIX EMCal below $p_T \lesssim 4$ GeV/c. This is the range in which the contribution from thermal direct photons is expected to be largest. A solution to this quandary is the measurement of virtual photons with small mass via their internal conversion in e^+e^- pairs [15]. Electrons and positrons are identified within PHENIX with a Ring Imaging Cherenkov detector and by matching the measured track momentum with the energy signal in the EMCal. e^+e^- pairs from external conversions in the detector material are removed by a cut on the orientation of the pair in the magnetic field. The combinatorial background is subtracted using a mixed-event technique. The remaining correlated background is subtracted with the aid of constructing like-sign pairs.

The internal conversion method exploits the fact that any source of real photons also is a source of virtual photons and that the rate of internal conversions and the mass distribution of the e^+e^- pairs is calculable within QED. The number of e^+e^- pairs per real photon is given by [16]

$$\frac{1}{N_\gamma} \frac{dN_{ee}}{dm_{ee}} = \frac{2\alpha}{3\pi} \frac{1}{m_{ee}} \sqrt{1 - \frac{4m_e^2}{m_{ee}^2}} \left(1 + \frac{2m_e^2}{m_{ee}^2}\right) S. \quad (3)$$

For hadron decays, *e.g.*, the π^0 Dalitz decay, $S = |F(m_{ee}^2)|^2 (1 - m_{ee}^2/M_h^2)^3$ where $F(m_{ee}^2)$ is the form factor and M_h the hadron mass. For a point-like process such as gluon Compton scattering ($q + g \rightarrow q + \gamma^* \rightarrow q + e^+ + e^-$) $S \approx 1$ for $p_T^{e^e} \gg m_{ee}$. The two cases are shown in Figure 4a.

At small masses $m_{ee} < 30$ MeV the mass distribution is to very good approximation independent of the source and the fraction of real direct photons can be expressed in terms of virtual photons, *i.e.*, $r \equiv \gamma_{\text{direct}}/\gamma_{\text{inclusive}} = (\gamma_{\text{direct}}^*/\gamma_{\text{inclusive}}^*)_{m_{ee} < 30 \text{ MeV}}$. At larger masses e^+e^- pairs

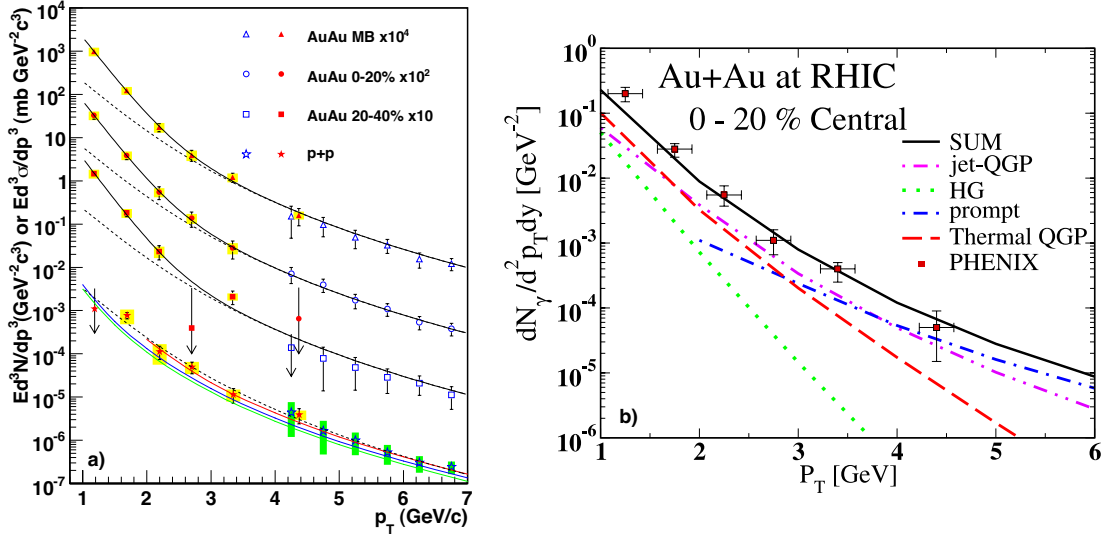


Figure 5: a) Invariant direct-photon cross sections (p+p) and yields (Au+Au) at $\sqrt{s_{NN}} = 200$ GeV [15]. The closed symbols are from the internal conversion method, the open symbols from EMCAL measurements. b) Comparison of the direct-photon spectrum in the 20% most central Au+Au collisions with a calculation from [2]

from hadronic decays are suppressed by the S factor and $m_{ee} < M_h$ holds. Thus, the background from π^0 Dalitz decays could be completely avoided by measuring virtual direct photons in the range $m_{ee} > M_{\pi^0}$. However, this comes at the expense of a loss in statistics as for every real direct photon there are only ~ 0.001 virtual direct photons with $m_{ee} > M_{\pi^0}$.

For a given p_T bin the direct-photon fraction r is determined as follows. First the mass distribution of e^+e^- pairs from hadronic decays f_{cocktail} with contributions from $\pi^0, \eta, \omega, \eta'$, and ϕ and the mass distribution for virtual direct photons f_{direct} are separately normalized to the data at $m_{ee} < 30$ MeV. Then r is extracted by fitting $f(m_{ee}) = (1 - r)f_{\text{cocktail}}(m_{ee}) + rf_{\text{direct}}(m_{ee})$ in the range $80 < m_{ee} < 300$ MeV (see Figure 4b).

The direct-photon spectra in p+p and Au+Au collisions at $\sqrt{s_{NN}} = 200$ GeV from the internal conversion method are shown in Figure 5 along with the EMCAL measurements. The p+p spectrum agrees with the NLO QCD calculation over the entire range $1 < p_T < 7$ GeV/c. The p+p data can be parameterized with $f_{p+p}(p_T) = A(1 + p_T^2/b)^{-n}$ (dashed line). For Au+Au the shape of the spectra differs significantly from the p+p spectrum and yields show a striking enhancement for $p_T \lesssim 2$ GeV/c with respect to $\langle T_{AB} \rangle \times f_{p+p}(p_T)$. A good fit of the Au+Au data can be obtained with $f_{Au+Au}(p_T) = \langle T_{AB} \rangle \times f_{p+p}(p_T) + B \exp(-p_T/T)$. The exponential shape of the enhancement in Au+Au is consistent with the assumption that the excess photons come from a thermal source. For the 20% most central Au+Au collisions the extracted slope parameter is $T = (221 \pm 23 \pm 18)$ MeV. In hydrodynamical models the initial temperature of the thermalized quark-gluon plasma is typically 1.5 to 3 times T . Thus, if the excess photons are of thermal origin the measured slope parameter T would indicate an initial temperature well above the critical temperature for the QGP phase transition.

Figure 5b shows a comparison of the Au+Au direct-photon data at low p_T with a calculation

which includes all the direct-photon sources discussed in section 1 [2]. The space-time evolution of the fireball is modeled with ideal hydrodynamics and an equation of state with a transition from a non-interacting quark-gluon plasma to a chemically equilibrated hadron resonance gas at a critical temperature of $T_c = 164$ MeV. The contribution from the pre-equilibrium phase is accounted for by starting the hydro-evolution early at $\tau_0 = 0.2$ fm/c. Assuming full equilibrium at $\tau_0 = 0.6$ fm/c corresponds to an initial temperature of $T_{\text{initial}} = 340$ MeV in this model. Another piece of evidence for the creation of a quark-gluon plasma is the fact that without photons from jet-plasma interactions the data cannot be described.

5 Conclusions

Direct photons at high p_T measured with the PHENIX EMCal played a crucial role in the discovery of jet quenching at RHIC. Neutral pions and other hadron in central Au+Au collisions are suppressed whereas direct photons up to $p_T \approx 14$ GeV/c scale with T_{AB} , *i.e.*, with the increase of the parton luminosity per collisions as expected from nuclear geometry. This strongly supports the interpretation of the high- p_T hadron suppression as being caused by the energy loss of quark and gluon jets in the created medium. Direct-photon hadron azimuthal correlations allow to better constrain the initial jet energy. The correlation data were compared to one particular jet quenching model which was only tuned to describe the single particle R_{AA} and agreement was found. A breakthrough is the measurement of low- p_T direct photons with the internal conversion method in p+p as well as in Au+Au collisions. The direct-photon spectrum in central Au+Au collisions spectra exhibits an enhancement above the scaled p+p spectrum for $p_T \lesssim 2$ GeV/c. The exponential shape of this enhancement and the slope parameter $T > T_c$ are consistent with the assumption that thermal photons from a QGP phase contribute significantly to this enhancement.

References

- [1] P. Stankus. *Ann. Rev. Nucl. Part. Sci.* 55 517 (2005).
- [2] C. Gale (2009). 0904.2184.
- [3] P. F. Kolb and U. W. Heinz (2003). [nucl-th/0305084](#).
- [4] Y. Aoki et al. (2009). 0903.4155.
- [5] M. Cheng et al. *Phys. Rev. D* 74 054507 (2006). [hep-lat/0608013](#).
- [6] K. Adcox et al. *Nucl. Phys. A* 757 184 (2005). [nucl-ex/0410003](#).
- [7] R. J. Fries, B. Muller, and D. K. Srivastava. *Phys. Rev. Lett.* 90 132301 (2003). [nucl-th/0208001](#).
- [8] B. G. Zakharov. *JETP Lett.* 80 1 (2004). [hep-ph/0405101](#).
- [9] S. S. Adler et al. *Phys. Rev. Lett.* 98 012002 (2007). [hep-ex/0609031](#).
- [10] S. S. Adler et al. *Phys. Rev. Lett.* 94 232301 (2005). [nucl-ex/0503003](#).
- [11] L. Aphcetchet et al. *Nucl. Instrum. Meth. A* 499 521 (2003).
- [12] M. L. Miller, K. Reygers, S. J. Sanders, and P. Steinberg. *Ann. Rev. Nucl. Part. Sci.* 57 205 (2007). [nucl-ex/0701025](#).
- [13] A. Adare et al. (2009). 0903.3399.
- [14] H. Zhang, J. F. Owens, E. Wang, and X.-N. Wang (2009). 0902.4000.
- [15] A. Adare et al. (2008). 0804.4168.
- [16] N. M. Kroll and W. Wada. *Phys. Rev.* 98 1355 (1955).